



Pulicaria gnaphalodes-assisted green synthesis of NiFe₂O₄@ZnO nanocomposites for sustainable remediation of an antibiotic from aqueous solution

Elham Derakhshani¹ · Ali Naghizadeh¹ · Sobhan Mortazavi-Derazkola¹ · Ali Yousefinia¹

Received: 28 December 2023 / Accepted: 16 March 2024 / Published online: 9 April 2024
© The Author(s) 2024

Abstract

In this study, the NiFe₂O₄@ZnO nanocomposite was synthesized in a simple, accessible and affordable method using *Pulicaria gnaphalodes* plant extract as a reducing agent. The structural characteristics of this nanocomposite were determined by transmission electron microscopy (TEM), X-ray diffraction, Fourier transform infrared spectroscopy, vibrating sample magnetometer, X-ray energy diffraction spectroscopy and dynamic light scattering. TEM micrograph confirmed the formation of spherical and cubic spinel ferrite with average dimensions of 75–85 nm. Some parameters such as pH, dose of NiFe₂O₄@ZnO nanocomposite, concentration of penicillin G and reaction time to reach optimal conditions were investigated. According to the results of the present research, the photocatalyst process along with the use of NiFe₂O₄@ZnO nanocomposite as an oxidizing agent is an effective method in degradation of the penicillin G antibiotic from aqueous solutions.

Keywords Photocatalytic · Nickel ferrite · Zinc oxide · Penicillin G · Green synthesis · Degradation

Introduction

Nanoscience and nanotechnology, which is rapidly growing and expanding in recent years, produces nanoparticles in the range of 1–100 nm by particle structure and size modification (Jamkhande et al. 2019). Today, the application of nanoparticles has increased in various fields of pharmaceuticals, textiles, medicine, printing, agriculture, environment and industry (Ren et al. 2019; Ardestani et al. 2020). Nanoparticles have characteristics such as large cross-sectional area, very small size, specific network order, crystalline shape, stability and high reactivity. These properties of nanoparticles have caused them to have various applications, one of the most important applications of which is the destruction and removal of toxic contaminants and organic pollutants from aqueous solutions and their transformation into harmless substances (Park et al. 2006; Ealia and Saravanakumar 2017). In the past decade, the use of spinel ferrites with the

general formula MFe₂O₄ has increased, where M in these magnetic nanoparticles is a divalent metal such as Ni, Fe, Mn, Co and Zn (Yelenich et al. 2015). Among these spinel ferrites, NiFe₂O₄ nanoparticles have attracted the attention of researchers due to their magnetic and catalytic properties, chemical and thermal stability, low cost and easy preparation, low toxicity and high absorption ability. Nickel ferrite nanoparticles due to the mentioned features are used in catalysts, drug delivery, medical diagnostics, information storage, pigments, electronic devices and as absorbents (Zandipak and Sobhanardakani 2016; Lingamdinne et al. 2017; Sanadi et al. 2021). These nanoparticles can be synthesized by various physical, chemical and biological methods, but physical and chemical methods are not very suitable for the synthesis of nanoparticles. Because the reaction is carried out in special and long conditions, and also due to the use of expensive and dangerous chemicals, they are not compatible with the environment (Senapati et al. 2012). Green synthesis of nanoparticles, which is performed using microorganisms (bacteria, fungal and algae) and plant extracts (extracts from leaves, roots, flowers, seeds and barks of different plants), can be an economic and valuable alternative to physical and chemical methods on a large scale (Ying et al. 2022). Plant extracts are commonly used as stabilizing, reducing and capping agents to control crystal growth (Din et al. 2018).

✉ Ali Naghizadeh
al.naghizadeh@yahoo.com

¹ Medical Toxicology and Drug Abuse Research Center (MTDRC), Birjand University of Medical Sciences (BUMS), Birjand, Iran

Pulicaria gnaphalodes is rich in phenolic compounds and has high antioxidant properties. This plant used for years in traditional Iranian medicine to treat heatstroke and severe diarrhea and as an anti-inflammatory. This plant, which belongs to the *Asteraceae* family, grows in hot and dry desert areas of Asia, Africa and Europe (Derakhshani et al. 2023). Today, the use of nanoparticles synthesized in a green way using plant extracts is considered as one of the newest methods to remove environmental pollutants.

Pharmaceuticals and personal care products (PPCPs) have wide applications in the fields of medicine, animal husbandry, industry, aquaculture, agricultural activities, cosmetic care and people's daily life and have been considered as emerging water pollutants. These products are a threat to humans and aquatic ecosystems due to their widespread use and poor purification by biological processes of wastewater (Wang and Wang 2016; Barceló and Petrovic 2007). PPCPs include several classifications, among which antibiotics are one of the most widely used categories in the prevention and treatment of infectious diseases in humans and animals (Kovalakova et al. 2020). Antibiotics are stable chemical compounds that after use, a small amount of them changes in the body, and a large percentage of them are excreted from the human and animal body unchanged and enter the environment through viruses or feces (Javadmoosavi et al. 2023). Also, pharmaceutical industry wastewater is one of the important industries in the introduction of antibiotics into the environment (Xian et al. 2010; Qin et al. 2021). The high concentration of antibiotics in the environment causes an increase in antibiotic resistance in pathogenic bacteria and as a result drug resistance in humans (Dimitrakopoulou et al. 2012). The antibiotic penicillin G (PG) ($C_{16}H_{17}N_2NaO_4S$), which is soluble in water, is one of the most commonly used antibiotics and belongs to the class of beta-lactam antibiotics (Ma et al. 2018). This antibiotic, which is used against vulnerable organisms, especially Gram-positive bacteria, destroys the cell wall of these bacteria by preventing the production of peptidoglycan (Peterson et al. 2012). Considering that, common processes in water and wastewater treatment are not able to remove and destroy these pollutants, method such as advanced oxidation processes (AOPs) should be used to eliminate them (Naghizadeh et al. 2017). Advanced oxidation processes are one of the practical methods for removing water-soluble pollutants, which is based on the production of hydroxyl free radicals using ozone, H_2O_2 , UV and a combination of them. These free radicals have a high power in destroying strong and toxic pollutants due to having free electron (Akbari et al. 2019; Derakhshani and Naghizadeh 2014). Photocatalytic degradation, as one of the advanced oxidation processes, is a sustainable, clean, environmentally friendly and economical method in energy consumption, and it can be used to remove high

concentrations of antibiotics in aqueous solutions (Gusain et al. 2019; Koe et al. 2020). In the present study, green synthesis of $NiFe_2O_4@ZnO$ nanocomposite using *Pulicaria gnaphalodes* was examined for photocatalytic degradation of PG in aqueous solution.

Materials and methods

Materials

At the first, penicillin G powder was purchased from Sigma-Aldrich, and then, penicillin G stock solution with a concentration of 500 mg/L was prepared using double-distilled water. Other chemicals used in this study include iron nitrate ($Fe(NO_3)_3 \cdot 9H_2O$), nickel chloride salt ($NiCl_2 \cdot 6H_2O$), sodium dodecyl sulfate (SDS) surfactant, zinc nitrate salt ($Zn(NO_3)_2 \cdot 6H_2O$), sodium hydroxide (NaOH), hydrochloric acid (HCl), methanol and ethanol were purchased from Merck (Germany). UV-C lamp (Philips, Poland) with a power consumption of 9 watts, radiation intensity of 282–294 W/m^2 , wavelength of 253.7 nm, diameter of 2 cm and length of 22 cm was installed and used in the center of the reactor.

Preparation of methanolic plant extract

For the synthesis of $NiFe_2O_4@ZnO$ nanocomposite, the *Pulicaria gnaphalodes* plant was collected from around the Birjand city (the capital of South Khorasan Province, Iran) and transported to the laboratory. This plant was washed three times with distilled water and then placed at room temperature to dry. To prepare the extract, some of the dried powder of the plant was contacted with methanol solution, and then, the solution was passed through Whatman No. 42 paper. A rotary vacuum evaporator (Hei zbad WB eoc, Germany) was used for methanol concentration and plant extract separation. The schematic of methanolic extract of *Pulicaria gnaphalodes* is shown in Fig. 1.

Biosynthesis of $NiFe_2O_4@ZnO$ nanocomposite

First, for the synthesis of nanocomposite $NiFe_2O_4$, 5 g of iron nitrate hexahydrate ($Fe(NO_3)_3 \cdot 9H_2O$) was added to 70 mL of deionized water and dissolved in water under nitrogen gas for 1 h. In another container, SDS surfactant (1:1 molar ratio to iron salt) was dissolved in 30 mL of distilled water and added to iron salt as a coating agent. The reaction was continued for 30 min under vigorous stirring at room temperature. Then, 1.47 g of nickel chloride salt ($NiCl_2 \cdot 6H_2O$) was added to the reaction solution and 2 M sodium hydroxide to increase the pH of the reaction to 12. After 2 h, the sediments obtained were washed and dried



Fig. 1 Schematic of methanolic extract of *Pulicaria gnaphalodes*

after centrifugation at room temperature for 24 h. NiFe₂O₄ nanocomposite was obtained by calcining the deposits at 600 °C for 3 h.

A molar ratio of 1:1 was used for the synthesis of NiFe₂O₄/ZnO nanoparticles. For this purpose, 0.5 g of NiFe₂O₄ nanoparticles was dispersed in 20 mL of distilled water for 30 min under ultrasonic conditions. Then, 1 g of zinc nitrate salt (Zn(NO₃)₂·6H₂O) was dissolved in 10 mL of distilled water and slowly added to the reaction solution together with the *Pulicaria gnaphalodes* plant extract at 45 °C. After 30 min, sodium hydroxide solution (2 M) was slowly added to the reaction (pH 12). The reaction continued for 2 h under magnetic stirring. Then, after washing and drying, the obtained precipitate was calcinated at 500 °C for 2 h. The schematic of NiFe₂O₄@ZnO green synthesis is shown in Fig. 2.

Results and discussion

Structural analysis

FT-IR analysis

FT-IR spectrum was used to identify of NiFe₂O₄@ZnO nanocomposites. FT-IR spectrum of biosynthesized NiFe₂O₄@ZnO nanocomposites is shown in Fig. 3. The stretching vibration band of Zn–O bonding was observed at 462 cm⁻¹ (Moradi et al. 2018). It can also be seen that the absorption bands at 473 and 582 cm⁻¹ are related to the metal–oxygen (M–O) vibration of the tetrahedral and octahedral sites of the spinel structure (Liu et al. 2013).

XRD analysis

The X-rays pattern displays the formation of the spinel phase structure of NiFe₂O₄ without any additional impurity peaks in Fig. 4. The diffraction peaks appeared at the diffraction angles 2θ = 30.295°, 35.686°, 37.330°, 43.375°, 53.820°, 57.377° and 63.015° which could be indexed based on

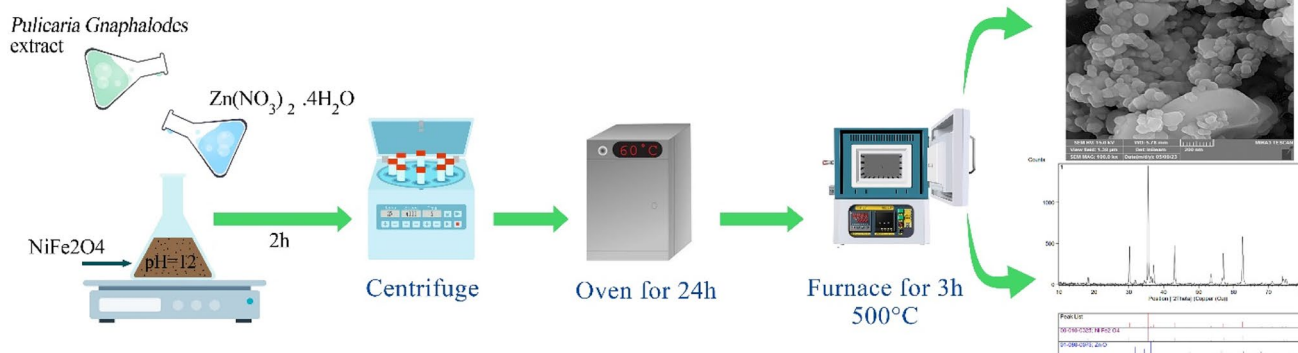


Fig. 2 Green synthesis of NiFe₂O₄@ZnO with *Pulicaria gnaphalodes* plant methanolic extract

Fig. 3 The FT-IR spectrum of NiFe₂O₄@ZnO nanocomposite

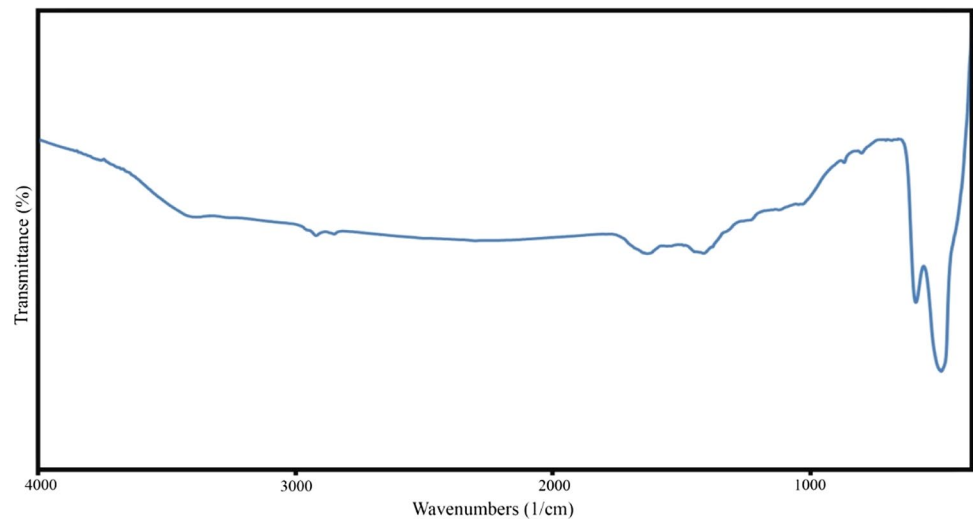
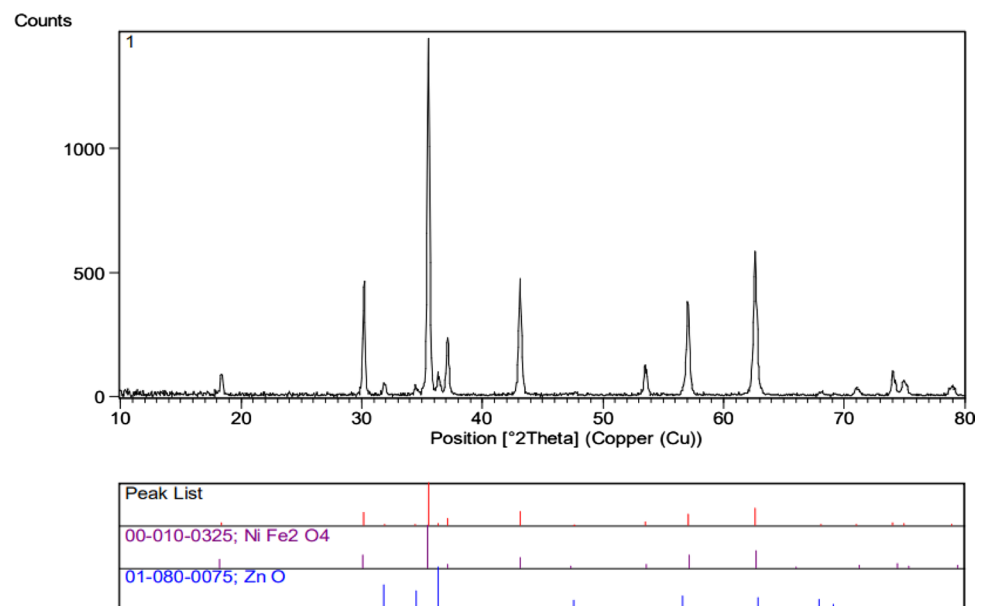


Fig. 4 The XRD pattern of NiFe₂O₄@ZnO nanocomposite



standard (JCPDS card No.74-2081) to (220), (311), (222), (400), (422), (511) and (440), respectively, correspond to spinel structure of NiFe₂O₄ (Bashir et al. 2020).

DLS analysis

Dynamic light scattering (DLS) and zeta-potential analysis were utilized to characterize the hydrodynamic size and surface charge of NiFe₂O₄@ZnO nanocomposites. The DLS graph of biosynthesized NiFe₂O₄@ZnO nanocomposites is shown in Fig. 5. The DLS results exhibited that the average hydrodynamic size of the NiFe₂O₄@ZnO nanocomposites was about 90–120 nm. The negative or positive charge on the surface of products prevents the aggregate of samples by repulsion of similar charges. The zeta-potential value was calculated to be −6.2 mV.

VSM analysis

Since the magnetic property of a catalyst is an essential parameter in separation and recovery processes (Ataei et al. 2021). The magnetic properties of the sample were analyzed by VSM analysis. The magnetic properties of NiFe₂O₄@ZnO were measured at room temperature and are shown in Fig. 6. According to the results, the magnetic saturation value for nanocomposite was 47 emug^{−1}. VSM analysis showed that the prepared nanocomposite has paramagnetic properties, and according to this analysis, it can be seen that the studied nanocomposite can be dispersed in water within a few minutes and separated using an external magnetic field. Then, it dispersed again with a small shake (Esmati et al. 2021).

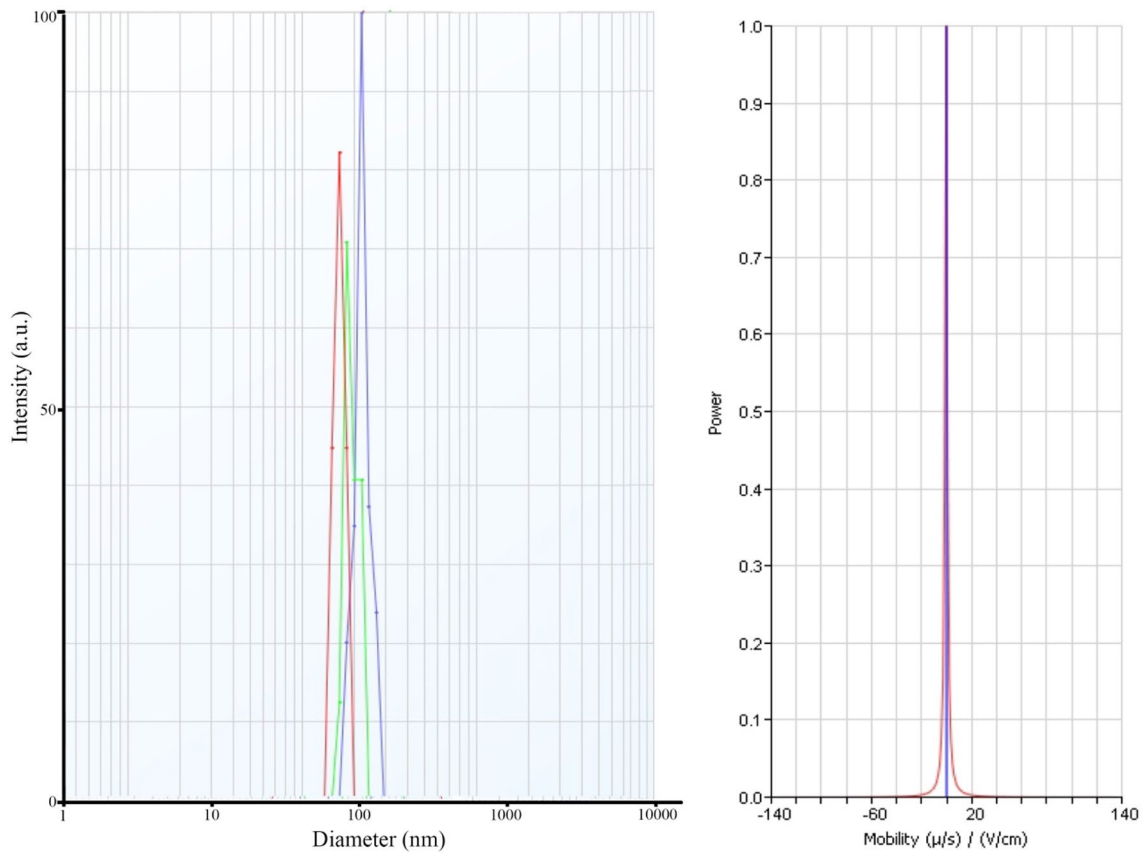


Fig. 5 The DLS analysis of NiFe₂O₄@ZnO nanocomposite

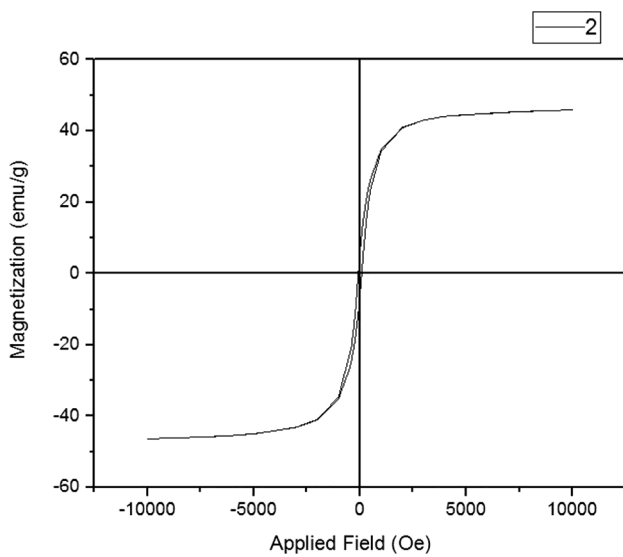


Fig. 6 The VSM pattern of NiFe₂O₄@ZnO nanocomposite

TEM analysis

In this study, the dimensions and structural characteristics of the NiFe₂O₄@ZnO nanoparticles were meticulously

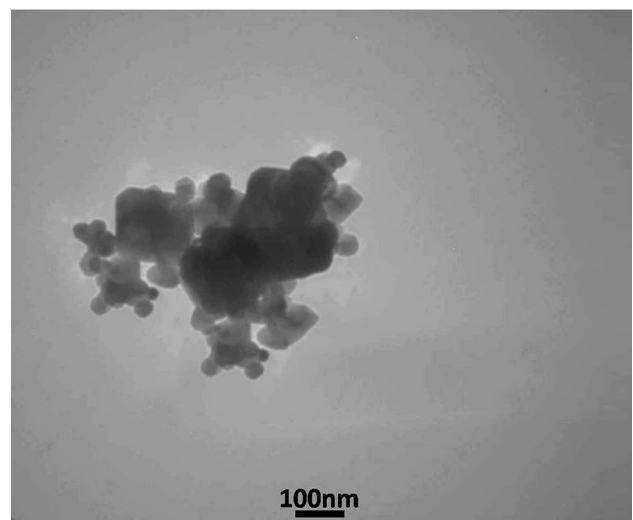


Fig. 7 The TEM micrograph of NiFe₂O₄@ZnO nanocomposite

examined using transmission electron microscopy (TEM), as depicted in Fig. 7. The TEM micrograph reveals distinct spherical and cubic morphologies of the synthesized nanoparticles. Notably, the dopant distribution on the NiFe₂O₄ substrate is discernible and well-defined. Upon closer

scrutiny, the size of the synthesized $\text{NiFe}_2\text{O}_4@\text{ZnO}$ nanoparticles can be reliably estimated to fall within the range of 75–85 nm. This observation underscores the meticulous control achieved during the synthesis process, confirming the desired morphology and size uniformity of the nanoparticles.

EDS mapping analysis

The investigation of the synthesized $\text{NiFe}_2\text{O}_4@\text{ZnO}$ nanoparticles through scanning electron microscopy included an elemental mapping analysis employing energy-dispersive spectroscopy (EDS). Figure 8 illustrates the EDS mapping spectrum of the $\text{NiFe}_2\text{O}_4@\text{ZnO}$ magnetic nanoparticles. The elemental mapping of $\text{NiFe}_2\text{O}_4@\text{ZnO}$ nanoparticles revealed a distinct presence and even distribution of nickel (Ni), iron (Fe) and zinc (Zn) elements, thereby providing conclusive evidence regarding the successful synthesis of magnetic $\text{NiFe}_2\text{O}_4@\text{ZnO}$ nanoparticles. This uniform distribution

underscores the precision and efficiency of the synthesis process. Furthermore, the absence of any detectable impurities in the synthesized nanoparticles, as indicated by the EDS results, further substantiates the purity and quality of the fabricated $\text{NiFe}_2\text{O}_4@\text{ZnO}$ nanoparticles. The overall findings strongly support the assertion that the synthesis process was indeed successful and devoid of any undesirable contaminants.

Photocatalyst experiments

pH_{ZPC}

Using pH_{ZPC} , the surface charge of the catalyst was investigated. To determine the pH_{ZPC} of the produced nanocomposite, 11 containers containing 50 mL of distilled water with different pHs (2, 3, 4, 5, 6, 7, 8, 9, 10, 11 and 12) were prepared. Then, a specific dose of nanoparticles was added to the solution. After 24 h, the results were

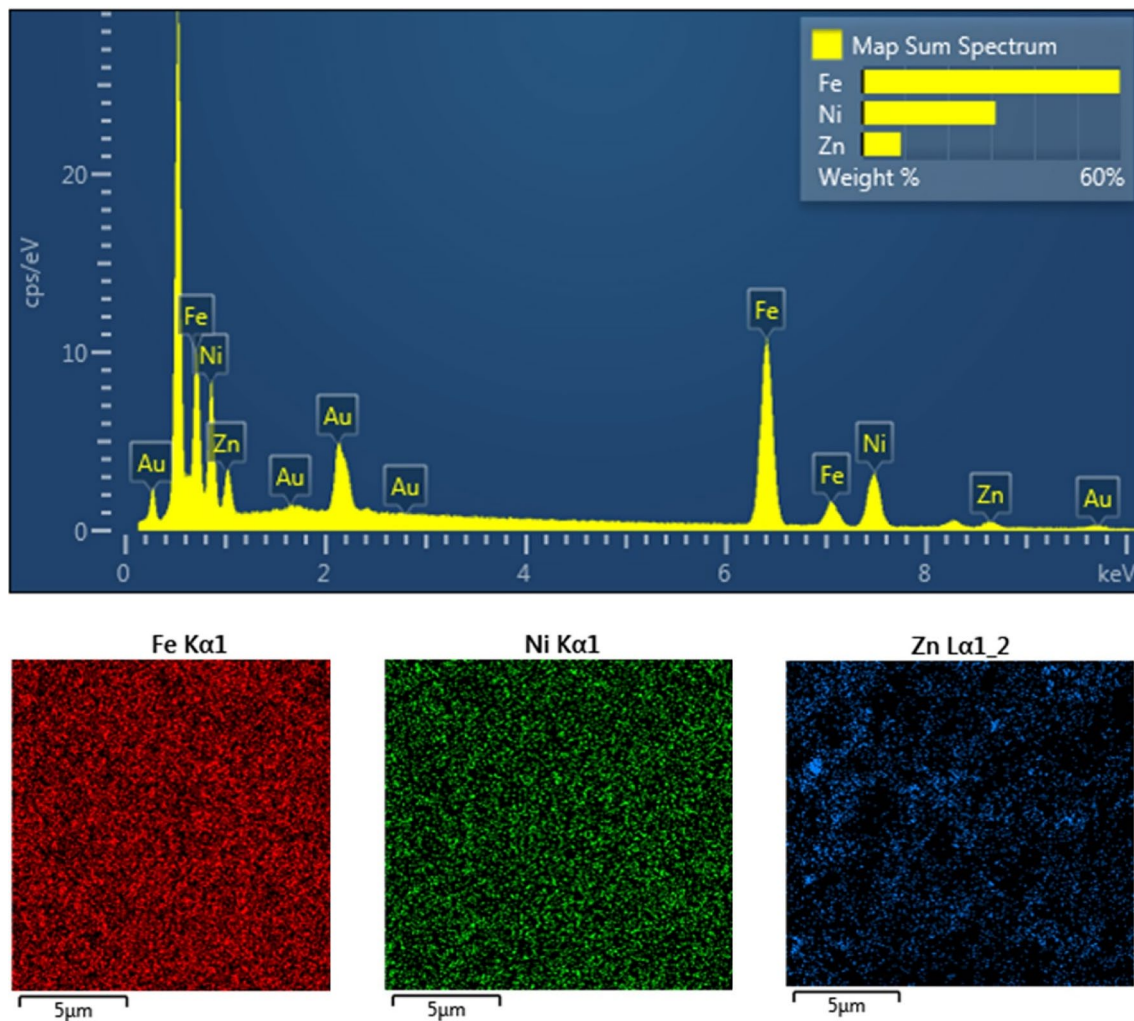


Fig. 8 The EDS analysis and mapping of $\text{NiFe}_2\text{O}_4@\text{ZnO}$ nanocomposite

recorded. The diagram of Fig. 9 shows the amount of surface charge of NiFe₂O₄@ZnO nanoparticles. As a result, at higher pH 6, the adsorbent surface has a negative charge, and as a result, ions with the opposite charge (positive ions) are easily adsorbed by nanocomposite. Also, at pH lower than 6, the surface charges of the catalyst become positive and negatively charged ions are absorbed faster.

This issue can be justified by the fact that at pH lower than pHzpc, the surface charge of the catalyst is positive, so the nanoparticles can react more effectively with the hydroxyl groups in the solution and increase the penicillin G removal efficiency. It can also be explained that in acidic pH, the holes produced by light irradiation on the catalyst surface act as the dominant oxidizing agent, these holes migrate to the catalyst surface in the valence band and interact with water molecules and ions. Hydroxyls react on the surface and produce hydroxyl radicals and hydrogen ions, which lead to the decomposition of pollutants adsorbed on the surface of the photocatalyst (Canle et al. 2017).

Determination of pH effect

The results of the studies show that pH directly affects radical production (Norzaee et al. 2017); as a result, it is considered an important factor in the photocatalyst process. According to pHzpc, for pH values lower than 6, the catalyst surface is often positively charged (h⁺ ions), and for pH values higher than 6, the catalyst surface is ignited by OH⁻ ions (Naghizadeh et al. 2020; Ghaemi et al. 2014). PG is a weak acid in water-soluble state (pKa=2.75) (Hossain and Dean 2008). As a result, if the pH of the solution is higher than the pKa value, the antibiotic PG tends to become anion. Also, if the pH is higher than 6, it will have a negative surface charge of the adsorbent and an anionic nature, and we can observe the electrostatic repulsion between the catalyst and PG. It is created to reduce the degradation of PG, but the experiments went against our expectations. According to Fig. 10, despite repeating the experiment, this nanoparticle showed that it has higher removal efficiency in alkaline environment.

Fig. 9 Diagram of pHzpc of NiFe₂O₄@ZnO synthesized by *Pulicaria gnaphalodes*

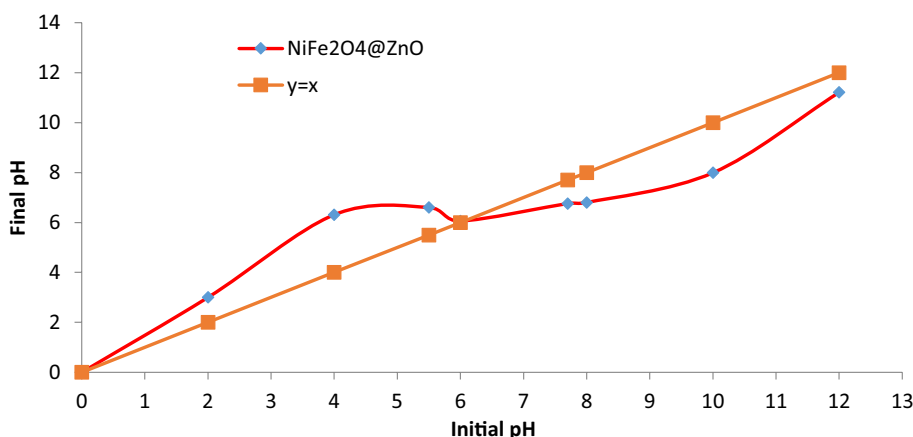
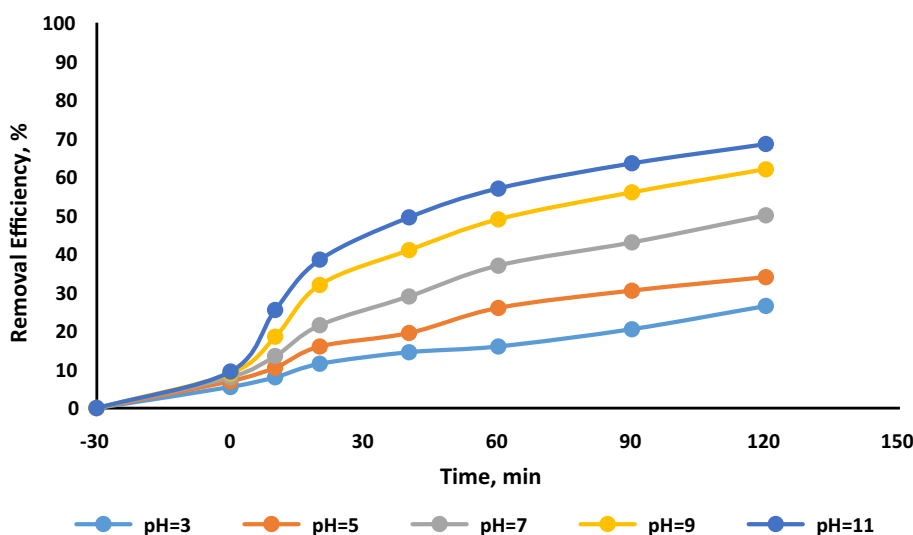


Fig. 10 Effect of reaction time and pH in photocatalytic degradation of PG by NiFe₂O₄@ZnO nanocomposite (C₀=20 mg/L, nanocatalyst dosage=0.6 g/L, T=25 °C)

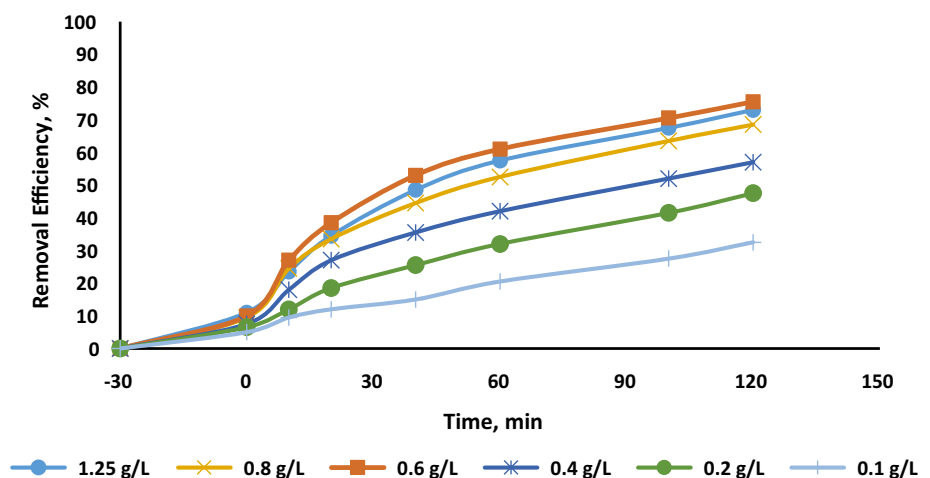


The pollutant concentration of 20 mg/L and the nanocatalyst dose of 0.6 g/L were considered at room temperature for the pH ranges of 3, 5, 7, 9 and 11, and the results showed a direct relationship between pH and removal efficiency, so that the highest the pollutant removal efficiency was related to pH 11, which is the most alkaline. The reason for this behavior can be explained that in the alkaline environment, there are more hydroxide ions (OH) on the surface of nanoparticles that are easily oxidized and form hydroxyl radicals (OH) with a very high oxidation potential, which increases that pollutants are destroyed. Also, the instability of the β -lactam ring in alkaline environments can be effective in further degrading the pollutant (Elmolla and Chaudhuri 2010).

Nanocatalyst dose effect

After determining the optimal pH in the previous step, the effect of catalyst dosage on PG degradation efficiency was tested in the range of 0.1–1.25 g/L, pollutant concentration of 20 mg/L at room temperature. According to the results that can be seen on the graph of Fig. 11 initially, with the increase in the dose of nanocomposite, the amount of pollutant removal has also increased, but for concentrations higher than 0.6 g/liter, the power of nanoparticle destruction has a downward trend. The reason for the upward trend in the graph can be explained by the active sites on the surface of the nanocatalyst, which increases the dose of nanoparticles, increases hydroxyl radicals and increases the pollutant degradation efficiency (Kamranifar et al. 2019) and can be the reason for its downward trend for concentrations higher than 0.6 g/L. The inability to penetrate UV light in the solution is due to the lack of the number of nanoparticles (Daneshvar et al. 2004).

Fig. 11 Effect of dose of $\text{ZnFe}_2\text{O}_4/\text{ZnO}$ nanocomposite in photocatalytic degradation of PG by $\text{NiFe}_2\text{O}_4/\text{ZnO}$ nanocomposite ($C_0=20$ mg/L, pH=9, $T=25$ °C)



Determination of the effect of PG concentration and contact time

The efficiency of the $\text{NiFe}_2\text{O}_4/\text{ZnO}$ degradation process can be impacted by two key factors: PG pollutant concentration and contact time. In this study, we investigated the effect of PG concentration (ranging from 10 to 150 mg/L) on its photocatalytic degradation at room temperature (other parameters were fixed in optimized values, pH = 11, catalyst dose 0.6 g/L). The graph of Fig. 12 displays the results, indicating a decrease in nanoparticle removal efficiency as PG concentration increases from 10 to 150 mg/L. As the concentration of pollutants increases, the efficiency of the removal process decreases. This decrease in efficiency can be attributed to several factors. For instance, the formation of OH radicals in the photocatalytic process remains constant for a fixed amount of catalyst dose.

As a result, the available OH radicals may not be sufficient to decompose high concentrations of penicillin G. Furthermore, increased concentration of pollutants leads to the absorption of light by antibiotic molecules, making them less exposed to UV photons (Derakhshani et al. 2024). In a study entitled "Photocatalytic Removal of PG Pollutant from Aqueous Solution with $\text{Fe}^{+3}\text{-TiO}_2$ Nanoparticles" which conducted by Dehghani et al., the results showed that the efficiency of antibiotic removal increased as the initial concentration of PG decreased (Dehghani et al. 2014). Based on the graphs shown in Figs. 10, 11 and 12, which were used to determine the optimal state of photocatalytic activity of the nanocatalyst, it can be concluded that all experiments had a contact time ranging from 0 to 120 min. The results indicate that there is a direct relationship between the increase in contact time and the amount of removal, as the number of OH radicals and positive generating holes increases with longer contact time. This is a predictable outcome. Although the slope of the graphs is higher in the first 20 min, it may be due to the active surfaces on the nanocatalyst rapidly saturating (Ghauch et al.

Fig. 12 Effect of PG concentration in photocatalytic degradation of PG by NiFe₂O₄@ZnO nanocomposite (C₀=20 mg/L, nanocatalyst dosage=0.6 g/L, pH=9, T=25 °C)

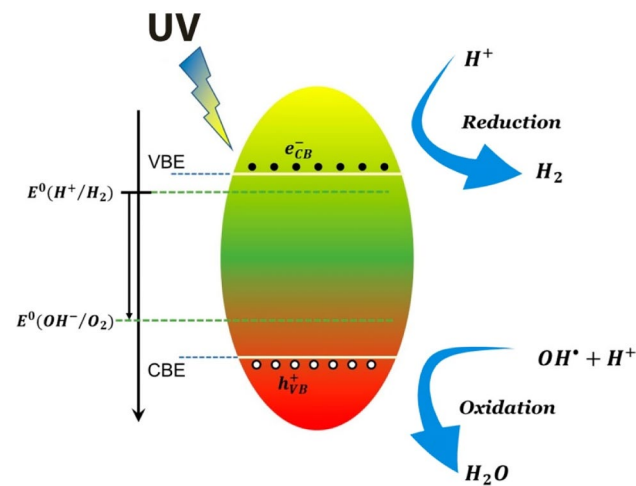
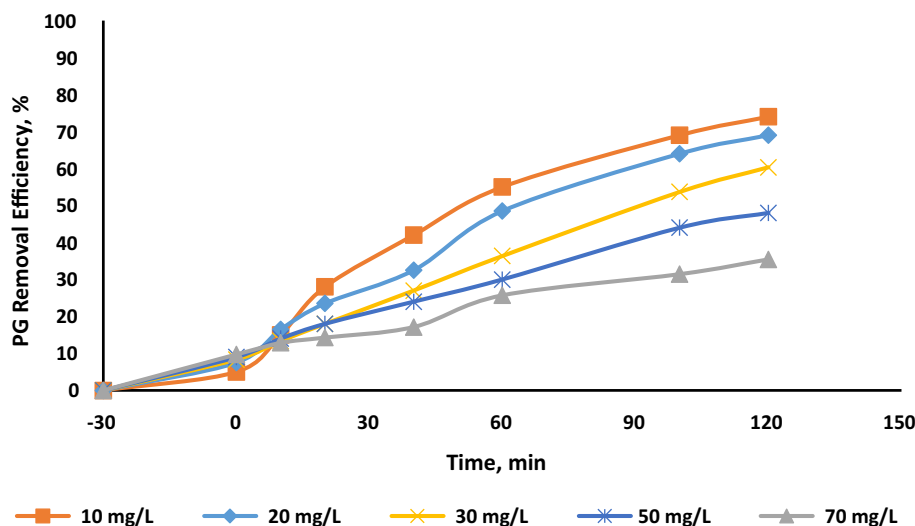


Fig. 13 The schematic of photocatalytic degradation of PG by NiFe₂O₄@ZnO

2009). A study entitled "Graphitic carbon nitride loaded on powdered mesoporous silica nanoparticles for photocatalytic tetracycline antibiotic degradation under UV-C light irradiation" was conducted in 2023. The study found that the highest removal efficiency occurred when the contact time was 120 min, which was the longest contact time tested in the experiment (Naghizadeh et al. 2023). The schematic of photocatalytic degradation of PG by NiFe₂O₄@ZnO is shown in Fig. 13.

Conclusion

This study investigated the synthesis of NiFe₂O₄@ZnO nanocomposite using methanolic extract of elder tree bark. Various analyses such as FT-IR, XRD, DLS, VSM, TEM and EDS were performed and reported to identify

the structure and elemental composition, which indicates the successful synthesis of magnetic nanocomposites with a diameter of 75–85 nm. Also, the synthesized magnetic nanoparticles were able to remove the penicillin G antibiotic in aqueous solutions under UV light, and the optimal conditions for doing it were also reported in the study.

Acknowledgements This article is part of the PhD thesis on Environmental Health Engineering that was approved by Birjand University of Medical Sciences (Tracking code: 456905). The authors want to acknowledge the never-ending support of the university.

Author contributions All authors contributed to the study conception and design. Material preparation, data collection and analysis were done by Elham Derakhshani and Ali Naghizadeh. The synthesis of the nanocomposite was done by Elham Derakhshani and Sobhan Mortazavi. The first draft of the manuscript was written by Elham Derakhshani and Ali Yousefinia. All authors read and approve the final manuscript.

Funding This work was supported by Birjand University of Medical Sciences.

Data availability All data generated or analyzed during this study are included in this published article.

Declarations

Conflict of interest All authors declare that they have no conflict of interests.

Ethical approval This article does not contain any studies with human participants or animals performed by any of the authors.

Consent to participate This section is “not applicable” for this study, as the study does not involve any human participants or their data or biological material.

Consent for publication All the authors mentioned in the manuscript have agreed to authorship, read and approved the manuscript and given consent for submission and subsequent publication of the manuscript.

Open Access This article is licenced under a Creative Commons Attribution 4.0 International License, which permits use, sharing, adaptation, distribution and reproduction in any medium or format, as long as you give appropriate credit to the original author(s) and the source, provide a link to the Creative Commons licence and indicate if changes were made. The images or other third-party material in this article are included in the article's Creative Commons licence, unless indicated otherwise in a credit line to the material. If material is not included in the article's Creative Commons licence and your intended use is not permitted by statutory regulation or exceeds the permitted use, you will need to obtain permission directly from the copyright holder. To view a copy of this licence, visit <http://creativecommons.org/licenses/by/4.0/>.

References

- Akbari F, Khodadadi M, Hossein Panahi A, Naghizadeh A (2019) Synthesis and characteristics of a novel $\text{Fe}_3\text{O}_4/\text{TiO}_2$ magnetic nanocomposites and its application in adsorption of humic acid from simulated wastewater: study of isotherms and kinetics. *Environ Sci Pollut Res* 26:32385–32396
- Ardestani MS, Bitarafan-Rajabi A, Mohammadzadeh P, Mortazavi-Derazkola S, Sabzevari O, Azar AD, Kazemi S, Hosseini SR, Ghoreishi SM (2020) Synthesis and characterization of novel 99mtc-dgc nano-complexes for improvement of heart diagnostic. *Bioorg Chem* 96:103572
- Ataei A, Mehrizad A, Zare K (2021) Photocatalytic degradation of cefazolin antibiotic using zeolite-supported CdS/CeO_2 Z-scheme photocatalyst: optimization and modeling of process by RSM and ANN. *J Mol Liq* 328:115476
- Barceló D, Petrovic M (2007) Pharmaceuticals and personal care products (Pcpcs) in the environment. *Anal Bioanal Chem* 387:1141–1142
- Bashir A, Matinise N, Sackey J, Kaviyarasu K, Madiba I, Kodseti L, Ezema F, Maaza M (2020) Investigation Of electrochemical performance, optical and magnetic properties Of NiFe_2O_4 nanoparticles prepared by a green chemistry method. *Phys e: Low-Dimens Syst Nanostruct* 119:114002
- Canle M, Pérez MIF, Santaballa JA (2017) Photocatalyzed degradation/abatement of endocrine disruptors. *Curr Opin Green Sustain Chem* 6:101–138
- Daneshvar N, Salari D, Khataee A (2004) Photocatalytic degradation of azo dye acid red 14 in water on ZnO as an alternative catalyst to TiO_2 . *J Photochem Photobiol A: Chem* 162:317–322
- Dehghani M, Nasserli S, Ahmadi M, Samaei MR, Anushiravani A (2014) Removal of penicillin G from aqueous phase By Fe^{3+} - $\text{TiO}_2/\text{UV-A}$ process. *J Environ Health Sci Eng* 12:1–7
- Derakhshani E, Naghizadeh A (2014) Ultrasound regeneration of multi wall carbon nanotubes saturated by humic acid. *Desalin Water Treat* 52:7468–7472
- Derakhshani E, Naghizadeh A, Mortazavi-Derazkola S (2023) Phyto-assisted synthesis of magnetic NiFe_2O_4 nanocomposite using the *Pulicaria gnaphalodes* methanolic extract for the efficient removal of an antibiotic from the aqueous solution: a study of equilibrium, kinetics, isotherms, and thermodynamics. *Aqua Water Infrastruct, Ecosyst Soc* 72:2035–2051
- Derakhshani E, Naghizadeh A, Mortazavi-Derazkola S (2024) Superior UVC light-mediated catalytic activity of a novel $\text{NiFe}_2\text{O}_4/\text{TiO}_2$ magnetic nanocomposite synthesized with green route using *Pulicaria gnaphalodes* plant extract for enhanced photocatalytic degradation of an antibiotic in water solution. *Appl Water Sci* 14:17
- Dimitrakopoulou D, Rethemiotaki I, Frontistis Z, Xekoukoulotakis NP, Venieri D, Mantzavinos D (2012) Degradation, mineralization and antibiotic inactivation of amoxicillin By $\text{UV-A}/\text{TiO}_2$ photocatalysis. *J Environ Manag* 98:168–174
- Din MI, Nabi AG, Rani A, Aihetasham A, Mukhtar M (2018) Single step green synthesis of stable nickel and nickel oxide nanoparticles from *Calotropis gigantea*: catalytic and antimicrobial potentials. *Environ Nanotechnol, Monit Manag* 9:29–36
- Ealia SAM, Saravanakumar MP (2017) A review on the classification, characterisation, synthesis of nanoparticles and their application. *Top Conf Ser: Mater Sci Eng* 263:032019
- Elmolla ES, Chaudhuri M (2010) Photocatalytic degradation of amoxicillin, ampicillin and cloxacillin antibiotics in aqueous solution using UV/TiO_2 And $\text{UV}/\text{H}_2\text{O}_2/\text{TiO}_2$ photocatalysis. *Desalination* 252:46–52
- Esmati M, Allahresani A, Naghizadeh A (2021) Synthesis and characterization of graphitic carbon nitride/mesoporous nano-silica (G-C3n4/Kcc-1) nanocomposite as a novel highly efficient and recyclable photocatalyst for degradation of antibiotic in aqueous solution. *Res Chem Intermed* 47:1447–1469
- Ghaemi M, Absalan G, Sheikhian L (2014) Adsorption characteristics of titan yellow and congo red on CoFe_2O_4 magnetic nanoparticles. *J Iran Chem Soc* 11:1759–1766
- Ghauch A, Tuqan A, Abou Assi H (2009) Antibiotic removal from water: elimination of amoxicillin and ampicillin by microscale and nanoscale iron particles. *Environ Pollut* 157:1626–1635
- Gusain R, Gupta K, Joshi P, Khatri OP (2019) Adsorptive removal and photocatalytic degradation of organic pollutants using metal oxides and their composites: a comprehensive review. *Adv Colloid Interface Sci* 272:102009
- Hossain MM, Dean J (2008) Extraction Of penicillin G from aqueous solutions: analysis of reaction equilibrium and mass transfer. *Sep Purif Technol* 62:437–443
- Jamkhande PG, Ghule NW, Bamer AH, Kalaskar MG (2019) Metal nanoparticles synthesis: an overview on methods of preparation, advantages and disadvantages, and applications. *J Drug Deliv Sci Technol* 53:101174
- Javadmoosavi S, Naghizadeh A, Mizwari Z, Mortazavi-Derazkola S (2023) Biosynthesis of novel $\text{NiFe}_2\text{O}_4/\text{X}$ ($\text{X} = \text{ZnO}$ And TiO_2) magnetic nanophotocatalyst toward the degradation pharmaceutical ceftriaxone sodium from aqueous solution under sunlight irradiation and antibacterial activity. *Ceram Int* 49:1351–1361
- Kamranifar M, Allahresani A, Naghizadeh A (2019) Synthesis and characterizations of a novel $\text{CoFe}_2\text{O}_4/\text{Cu}$ magnetic nanocomposite and investigation of its efficiency for photocatalytic degradation of penicillin G antibiotic in simulated wastewater. *J Hazard Mater* 366:545–555
- Koe WS, Lee JW, Chong WC, Pang YL, Sim LC (2020) An Overview Of photocatalytic degradation: photocatalysts, mechanisms, and development of photocatalytic membrane. *Environ Sci Pollut Res* 27:2522–2565
- Kovalakova P, Cizmas L, McDonald TJ, Marsalek B, Feng M, Sharma VK (2020) Occurrence and toxicity of antibiotics in the aquatic environment: a review. *Chemosphere* 251:126351
- Lingamdinne LP, Choi Y-L, Kim I-S, Yang J-K, Koduru JR, Chang Y-Y (2017) Preparation and characterization of porous reduced graphene oxide based inverse spinel nickel ferrite nanocomposite for adsorption removal of radionuclides. *J Hazard Mater* 326:145–156
- Liu H, Wu J, Min JH, Zhang X, Kim YK (2013) Tunable synthesis and multifunctionalities Of $\text{Fe}_3\text{O}_4/\text{ZnO}$ hybrid core-shell nanocrystals. *Mater Res Bull* 48:551–558
- Ma Q, Zhang H, Guo R, Li B, Zhang X, Cheng X, Xie M, Cheng Q (2018) Construction of CuS/TiO_2 nano-tube arrays photoelectrode

- and its enhanced visible light photoelectrocatalytic decomposition and mechanism of penicillin G. *Electrochim Acta* 283:1154–1162
- Moradi S, Taghavi Fardood S, Ramazani A (2018) Green synthesis and characterization of magnetic $\text{NiFe}_2\text{O}_4/\text{ZnO}$ nanocomposite and its application for photocatalytic degradation of organic dyes. *J Mater Sci: Mater Electron* 29:14151–14160
- Naghizadeh A, Momeni F, Derakhshani E (2017) Efficiency of ultrasonic process in regeneration of graphene nanoparticles saturated with humic acid. *Desal Water Treat* 70:290–293
- Naghizadeh A, Mohammadi-Aghdam S, Mortazavi-Derazkola S (2020) Novel $\text{CoFe}_2\text{O}_4/\text{ZnO}-\text{CeO}_2$ ternary nanocomposite: sonochemical green synthesis using crataegus microphylla extract, characterization and their application in catalytic and antibacterial activities. *Bioorg Chem* 103:104194
- Naghizadeh A, Etemadnia T, Derakhshani E, Esmati M (2023) Graphitic carbon nitride loaded on powdered mesoporous silica nanoparticles for photocatalytic tetracycline antibiotic degradation under Uv-C light irradiation. *Res Chem Intermed* 49:1165–1177
- Norzade S, Bazrafshan E, Djahed B, Kord Mostafapour F, Khaksefidi R (2017) Uv Activation of persulfate for removal of penicillin G antibiotics in aqueous solution. *Sci World J*. <https://doi.org/10.1155/2017/3519487>
- Park J-Y, Lee Y-J, Jun K-W, Baeg J-O, Yim DJ (2006) Chemical synthesis and characterization of highly oil dispersed Mgo nanoparticles. *J Ind Eng Chem* 12:882–887
- Peterson JW, Petrasky LJ, Seymour MD, Burkhart RS, Schuiling AB (2012) Adsorption and breakdown of penicillin antibiotic in the presence of titanium oxide nanoparticles in water. *Chemosphere* 87:911–917
- Qin K, Zhao Q, Yu H, Xia X, Li J, He S, Wei L, An T (2021) A Review of bismuth-based photocatalysts for antibiotic degradation: insight into the photocatalytic degradation performance. *Pathw Relevant Mech Environ Res* 199:111360
- Ren Y-Y, Yang H, Wang T, Wang C (2019) Bio-synthesis of silver nanoparticles with antibacterial activity. *Mater Chem Phys* 235:121746
- Sanadi K, Rathod K, Gaur M, Powar R, Parale V, Patil R, Burungale S, Mali A (2021) Uv light-activated photocatalytic degradation of rhodamine B dye and suzuki cross-coupling reaction by Ni ferrite catalyst synthesized by sol-gel auto-combustion method. *Bull Mater Sci* 44:1–8
- Senapati S, Syed A, Moez S, Kumar A, Ahmad A (2012) Intracellular Synthesis of gold nanoparticles using alga *Tetraselmis Kochinensis*. *Mater Lett* 79:116–118
- Wang J, Wang S (2016) Removal of pharmaceuticals and personal care products (Pcpcs) from wastewater: a review. *J Environ Manag* 182:620–640
- Xian Q, Hu L, Chen H, Chang Z, Zou H (2010) Removal of nutrients and veterinary antibiotics from swine wastewater by a constructed macrophyte floating bed system. *J Environ Manag* 91:2657–2661
- Yelenich O, Solopan S, Greneche J-M, Belous A (2015) Synthesis And properties MFe_2O_4 (M= Fe, Co) nanoparticles and core-shell structures. *Solid State Sci* 46:19–26
- Ying S, Guan Z, Ofoegbu PC, Clubb P, Rico C, He F, Hong J (2022) Green synthesis of nanoparticles: current developments and limitations. *Environ Technol Innov* 26:102336
- Zandipak R, Sobhanardakani S (2016) Synthesis Of NiFe_2O_4 nanoparticles for removal of anionic dyes from aqueous solution. *Desalin Water Treat* 57:11348–11360

Publisher's Note Springer Nature remains neutral with regard to jurisdictional claims in published maps and institutional affiliations.